

ChemComm

Accepted Manuscript



This is an Accepted Manuscript, which has been through the Royal Society of Chemistry peer review process and has been accepted for publication.

Accepted Manuscripts are published online shortly after acceptance, before technical editing, formatting and proof reading. Using this free service, authors can make their results available to the community, in citable form, before we publish the edited article. We will replace this Accepted Manuscript with the edited and formatted Advance Article as soon as it is available.

You can find more information about Accepted Manuscripts in the [author guidelines](#).

Please note that technical editing may introduce minor changes to the text and/or graphics, which may alter content. The journal's standard [Terms & Conditions](#) and the ethical guidelines, outlined in our [author and reviewer resource centre](#), still apply. In no event shall the Royal Society of Chemistry be held responsible for any errors or omissions in this Accepted Manuscript or any consequences arising from the use of any information it contains.



Journal Name

COMMUNICATION

Probabilistic mapping of single molecule junction configurations as a tool to achieve desired geometry of asymmetric tripodal molecules.

Received 00th January 20xx,
Accepted 00th January 20xx

DOI: 10.1039/x0xx00000x

www.rsc.org/

Viliam Kolivoška,^{a†} Jakub Šebera,^{a†} Táňa Sebechlebská,^{ab} Marcin Lindner,^{c‡} Jindřich Gasior,^a Gábor Mészáros,^d Marcel Mayor,^{cef} Michal Valášek^{*c} and Magdaléna Hromadová^{*a}

Four molecules containing identical tripodal anchor and *p*-oligophenylene molecular wire of increasing length were used to demonstrate tuning of the asymmetric molecular junction to desired geometry by probabilistic mapping of single molecule junction configurations in the scanning tunnelling microscopy break junction experiment.

Understanding the charge transport mechanism at single molecule level is regarded as an essential requirement for the realization of molecular electronic devices.^{1,2} Break-junction techniques derived from scanning tunnelling microscopy (STM) represent the most widely used experimental approach to investigate the charge transport in individual molecules.^{3–5} The conductance of a single molecule junction can change significantly due to changes in the contact geometry and configuration of molecules within the molecular junction (MJ).⁶ Therefore, repeated measurements are required to determine the most probable single molecule conductance value by a statistical approach.

Multipodal platforms^{7,8} are recently engineered molecular architectures proposed to serve as geometrically well-defined bases for functional elements in molecular electronic applications.^{9,10} Cyclohexane trithiol,^{11,12} adamantane tri-

thiol,^{13,14} triazatriangulene,^{15,16} trioxatriangulene,¹⁷ tris(azobenzyl)amine,¹⁸ spirobifluorene,^{19–21} tetraphenylsilane²² and tetraphenylmethane^{23–25} tripodal platforms were synthesized to secure an attachment of a molecule to an electrode by three anchoring groups. First single molecule charge transport measurements were reported for symmetric molecules containing the same tripodal anchor on both ends.^{25,26} Single molecule charge transport studies within asymmetric molecules containing one multipodal platform with covalently attached functional element (molecular wire) have been reported only recently.^{20,21,24,27} A series of molecular wires consisting of a tetraphenylmethane tripodal platform and phenylene repeating units terminated by CN group have been studied in terms of the optimal anchor group position (three thiol groups in *meta* or *para* position relative to the sp³ hybridized carbon atom). It was shown that *meta* anchored tripod forms more compact self-assembled monolayers on Au(111) surfaces compared to *para* substituted platforms.^{24,27} However, the single molecule conductance obtained by break junction technique was independent of the molecular wire length for both tripods. This was attributed to the fact that in the derivatives containing CN-terminated molecular wire the conductance path involves two thiolate groups of the tripod rather than the wire itself.²⁷

Charge transport studies in asymmetric MJs often involve several conduction pathways and a great care must be taken to understand all of them and to tune the MJ geometry to the desired one.^{20,27,28} In this communication we demonstrate tuning of the charge transport pathway in asymmetric molecules through the backbone of a wire on a series of molecules **1** to **4** having identical *meta* tripodal platform covalently linked to a *p*-oligophenylene molecular wire of increasing length terminated by a thiol group (Chart 1). Such molecules differ from previously reported ones²⁷ in their ability to promote wire-based charge transport. Our strategy towards controlled asymmetric molecular junctions with tripodal contact geometry involves combined systematic theoretical and experimental approach described below.

^a J. Heyrovský Institute of Physical Chemistry of the Czech Academy of Sciences, Dolejškova 3, 18223 Prague, Czech Republic. E-mail: hromadom@jh-inst.cas.cz

^b Department of Physical and Theoretical Chemistry, Faculty of Natural Sciences, Comenius University in Bratislava, Mlynská Dolina, Ilkovičova 6, 84215 Bratislava 4, Slovakia.

^c Karlsruhe Institute of Technology (KIT), Institute of Nanotechnology, P. O. Box 3640, 76021 Karlsruhe, Germany. E-mail: michal.valasek@kit.edu

^d Research Centre for Natural Sciences, HAS, Magyar tudósok krt. 2, H-1117 Budapest, Hungary.

^e Department of Chemistry, University of Basel, St. Johanns-Ring 19, 4056 Basel, Switzerland.

^f Lehn Institute of Functional Materials, School of Chemistry, Sun Yat-Sen University, Guangzhou 510275, China.

[†] These authors contributed equally.

[‡] Present address: Institute of Organic Chemistry, Polish Academy of Sciences, Kasprzaka 44/52, 01-224 Warsaw, Poland

[§] Electronic Supplementary Information (ESI) available: Synthesis and characterization of tetraphenylmethane derivatives **1** to **4** and their precursors, STM measurements for **1** to **4**, computational details, summary of experimental and theoretical charge transport characteristics. See DOI: 10.1039/x0xx00000x

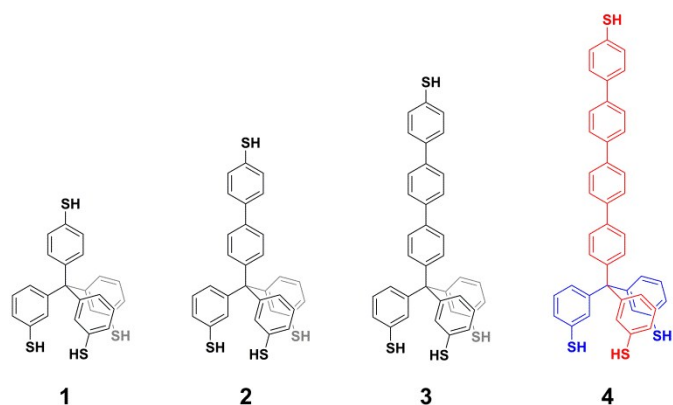


Chart 1. Chemical structures for molecules **1**, **2**, **3** and **4**. Blue and red color indicates two principal conduction pathways.

Synthetic procedures and full characterization of compounds **1** to **4** are given in the Supporting Information (SI). STMBJ technique was used for charge transport studies, where two gold electrodes were repeatedly brought in and out of contact in a solution of selected molecule, while current was measured as a function of the distance between electrodes. All STMBJ measurements were carried out in mesitylene solvent at ambient temperature using constant bias voltage $\Delta E = 130$ mV between the electrodes. Current–distance retraction curves were measured in a wide dynamic range²⁹ enabling detection of the gold–gold atomic contact as well as of the metal–molecule–metal junction conduction in the same curve. Up to 4000 individual current–distance curves were collected for each compound. They were first converted to conductance–distance curves using Ohm's law ($G = I/\Delta E$) and further processed statistically without any data selection generating 1D conductance, 2D conductance–distance and plateau length histograms. Detailed description of the histogram construction has been reported elsewhere.²⁰ Additional experimental details are given in the SI.

Figure 1 shows 1D conductance histograms for MJIs containing single molecules **1** to **4**. Peak at $\log(G/G_0) = 0$ corresponds to the gold–gold atomic contact, whereas features between $-6.2 < \log(G/G_0) < -2.5$ indicate true single molecule conduction. All members of the investigated series show a high conductance G_H peak (blue) centred between $-5 < \log(G/G_0) < -3$. Compounds **2** to **4** show another peak (red) at more negative $\log(G/G_0)$ values that will be referred to as low conductance G_L . All experimental conductance–distance curves were transformed to 2D conductance–distance histograms that report the most probable $\log(G/G_0)$ versus Δz values. Figure 2 shows such 2D histograms for molecules **1** to **4** highlighting the weighted average values of $[\log(G_H/G_0); \Delta z]$ pairs as blue traces and $[\log(G_L/G_0); \Delta z]$ pairs as red traces. Insets in Fig. 2 show plateau length histograms constructed at constant $\log(G/G_0) = -6.2$ value. Further details on the data treatment are reported in the SI. Blue peak in the inset represents the most probable plateau length Δz^* for high conductance value G_H of molecule **1**. Red peak represents the most probable plateau length for low conductance values G_L of molecules **2** to **4**, respectively. Black peak for molecules **2** to **4** gives either the junction length in the absence of molecules or

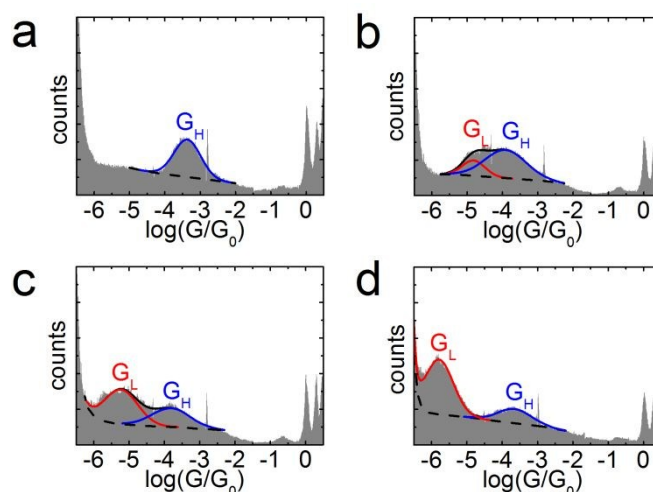


Fig. 1. 1D conductance histograms for molecules **1** (a), **2** (b), **3** (c) and **4** (d) with high conductance peak G_H (blue) and low conductance peak G_L (red) features. Signal below $\log(G/G_0) = -6.2$ corresponds to the noise level observed also in the absence of molecules.

for MJIs in the presence of G_H feature. Experimental MJ length was calculated from plateau length histograms as $z_{\text{exp}} = \Delta z^* + z_{\text{corr}}$, where $z_{\text{corr}} = 0.4$ nm represents the correction for a snap-back distance.²⁰ Summary of all experimental $\log(G_H/G_0)$, $\log(G_L/G_0)$ and z_{exp} values is given in Table S1 of the SI. Data show that the experimental junction length z_{exp} corresponding to G_L conductance feature increases with increasing length of the molecule. Furthermore, height of the low conductance peak G_L in Fig. 1 increases with increasing molecular wire length at the expense of G_H peak indicating a preferential formation of G_L type of molecular junction. Therefore, we have analysed individual conductance–distance traces in terms of the appearance of G_H and G_L features in the entire data sets for molecules **1** to **4**. Figure 3 shows representative conductance–distance traces obtained during the STMBJ experiment for molecules **1** to **4**.

Overall, four types of individual conductance–distance curves

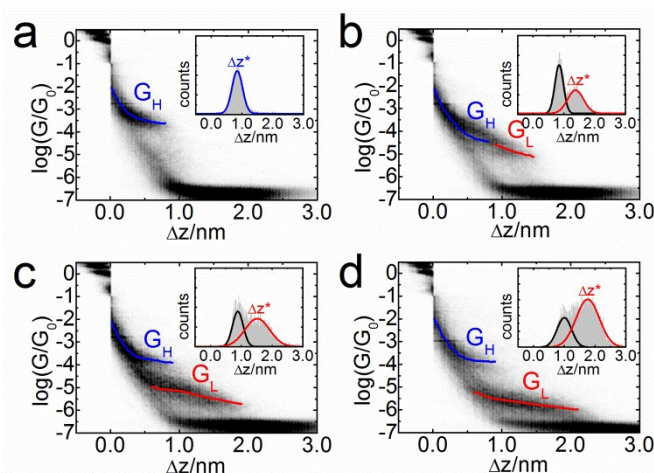


Fig. 2. 2D conductance–distance histograms for molecules **1** (a), **2** (b), **3** (c) and **4** (d), respectively. Inset shows corresponding plateau length histogram, where blue and red peaks represent G_H and G_L plateau length distribution, respectively. Black peak in the inset indicates junction length in the absence of G_L feature.

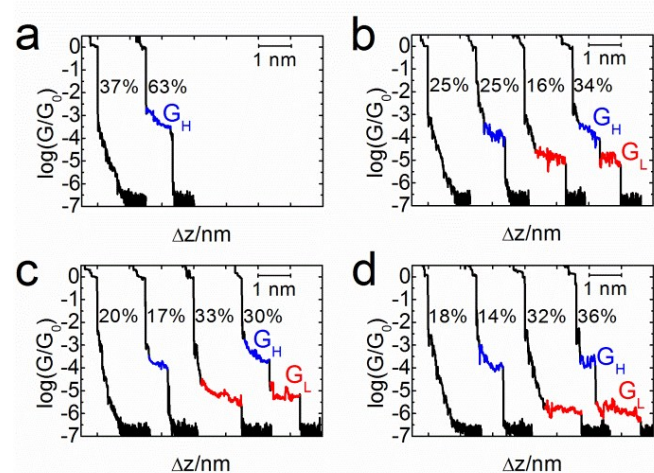


Fig. 3. Representative examples of conductance–distance curves for molecules **1** to **4** with probability P_j of their occurrence in the data set.

were observed representing junction without a molecule (black curve) showing only exponentially decreasing tunnelling current; junction with a single molecule showing a high conductance plateau (black–blue), low conductance plateau (black–red) and both (high and low) conductance plateaus. A value of the junction formation probability P_j is reported next to each curve as a percentage of the manually selected type of trace(s) within the entire set of experimentally–obtained conductance–distance traces. Fig. 3 shows that with increasing number of *p*-phenylene units n (see Chart 1 for structures of molecules **1** to **4**) the P_j value of curves showing low conductance G_L feature increases. This trend is also visible in Fig. 1 as G_L peak increases in height compared to G_H one. Indeed, the P_j value of curves showing high conductance G_H feature in Fig. 3 decreases with increasing number of *p*-phenylene units n .

Charge transport in single molecule junctions of **1** to **4** was analysed further theoretically by combining density functional theory (DFT) and non-equilibrium Green's function (NEGF) formalism. Computational details are in the Section 4 of the SI. Two possible scenarios for MJ configuration were considered. First one is called a platform configuration and represents charge transport through the tetraphenylmethane platform. The second one is named a tower configuration and accounts for the charge transport through a principal *p*-phenylene-based molecular axis. Chart 1 outlines these two conductance pathways for molecule **4** in blue (platform) and red (tower) colour.

Theoretical calculations employed either four thiolate anchors (tower case) or two thiolates of the tripod (platform case). An example of the resulting geometry optimized MJ configurations for molecule **4** is shown for platform configuration in Fig. 4a and for tower configuration in Fig. 4b. Summary of all geometry optimized MJ configurations for molecules **1** to **4** is provided in the SI. These configurations were used for the determination of the energy dependent transmission functions $\tau(\epsilon)$, from which theoretical G values for platform (G_P) and tower (G_T) configurations were calculated. These are represented by grey dotted lines in Fig. 4c, whereas

experimentally-obtained G_H and G_L values are shown as blue squares and red circles, respectively. Transmission functions $\tau(\epsilon)$ and theoretical conductance values for both sets of MJ configurations are summarized in Table S1 and in Section 5 of the SI. Transporting orbitals for each MJ configuration are shown in Section 7 of the SI. For both tower and platform MJ configurations, the Fermi level ϵ_F of the electrode lies closer to HOMO than to LUMO. This indicates that occupied orbitals are responsible for the charge transport.

Experimental MJ length z_{exp} increases with increasing number of *p*-phenylene units (see Fig. 4d) and is associated with low conductance values G_L . It is in very good agreement with theoretically obtained L_T values.

Figure 4e shows graph of the probability P_j of the tower MJ formation as a function of the number of phenylene units in the molecular wire backbone. Even though it is impossible to distinguish between G_H and G_L features for molecule **1** (thus we labelled it as G_H only) this is not the case for molecules **2** to **4**, where probability of the tower MJ configuration increases with increasing molecular wire length n . For molecule **4** we achieved 68% probability for the junction formation corresponding to tower configuration and only 14% corresponding to platform configuration. The rest represented junctions without any molecules. Thus, almost 83% of events

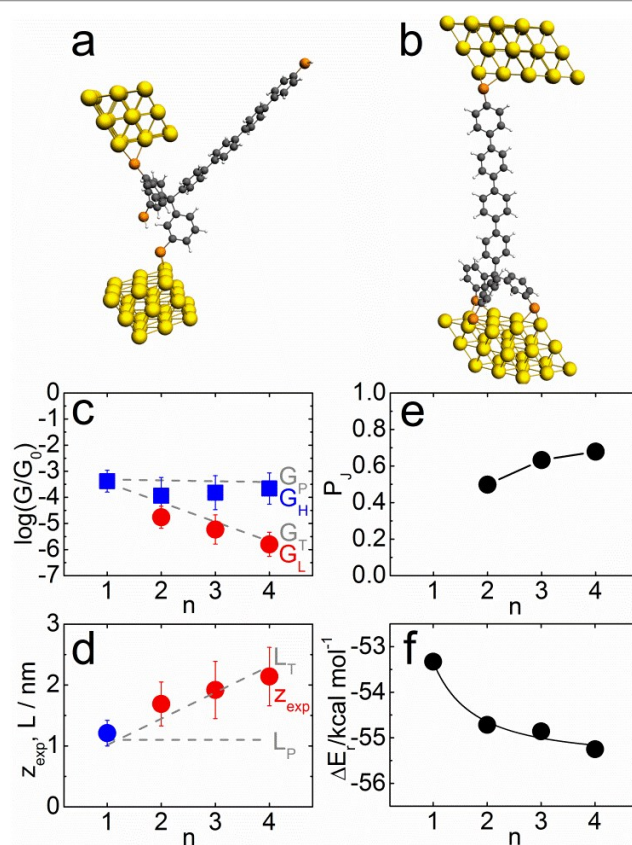


Figure 4. Example of (a) platform and (b) tower configurations for MJ of molecule **4**. Summary of the (c) $\log(G/G_0)$ values, (d) z_{exp} junction length values, (e) junction formation probability P_j values for G_L feature of molecules **2** to **4**, and (f) reaction energy ΔE , for transition from platform to tower MJ configuration, respectively. G_H (blue squares) and G_L (red circles) are experimental G values, G_P and G_T are theoretical G values, L_P and L_T are theoretical MJ length values for platform and tower configurations.

leading to junctions bridged by a molecule **4** were those with tower configuration. The characteristic plateau length of the G_L feature also increases with n . Thus in a dynamic system of molecules **1** to **4** an increase of the p -oligophenylene backbone promotes a contact by three thiolate groups of the tripodal platform (see Fig. 4b). Ultimately, by increasing the length of the p -oligophenylene wire one can steer the orientation of the asymmetric tripodal molecule to desired tower contact geometry inside the molecular junction (see Fig. 4e).

This behaviour was rationalized by an analysis of the energetics of tower and platform MJ configurations for molecules **1** to **4**. The electronic energies of tower (E_T) and platform (E_P) configurations were obtained by Turbomole program with DFT functional PBE (for further computational details see Section 4 of the SI). Then, the reaction energy ΔE_r for a process of transformation of the platform (P) to tower (T) junction configuration was computed as a function of n . The following reaction $P \rightleftharpoons T + H_2$ was considered, in which two SH groups of the platform are being transformed to thiolates and one hydrogen molecule. A graph of the reaction energies ΔE_r for molecular wires of different lengths is shown in Fig. 4f (for values of the electronic energies of the reactant and products see Table S4 of the SI). It demonstrates that the reaction energy for the above-mentioned process becomes more negative as the molecular wire length increases explaining preferential stabilization (higher probability) of the tower configuration with increasing molecular wire length which was observed experimentally. This stabilization can be explained by changes in the electronic structure of the molecule within the MJ (for further details see Section 9 of the SI).

In summary, we have successfully demonstrated control over the contact geometry of the asymmetric MJ by molecular design, namely by increasing the molecular wire length. An increase in the probability of tower configuration with increasing number of phenylene units was verified by the probabilistic mapping of single molecule junction configurations. We have shown that a rigid molecular tripod bearing sufficiently long molecular wire has favourable arrangement in the MJ, which allows further incorporation of sterically demanding molecular electronic elements into the molecular electronics architecture.

We acknowledge the financial support by Czech Science Foundation (16-07460Y, 18-04682S), Czech Academy of Sciences (MTA-16-02, RVO: 61388955), Hungarian Academy of Sciences OTKA (K112034, K119797), Baden-Württemberg Stiftung (Functional Nanostructures) and the Helmholtz Research Program (Science and Technology of Nanosystems).

Conflicts of interest

There are no conflicts to declare.

Notes and references

- J. C. Cuevas and E. Scheer, *Molecular electronics: An introduction to theory and experiment*; World Scientific Publishing Co. Pte. Ltd.: Singapore, 2010.
- D. Xiang, X. Wang, C. Jia, T. Lee and X. Guo, *Chem. Rev.* 2016, **116**, 4318.
- B. Xu and N. J. Tao, *Science* 2003, **301**, 1221.
- I. V. Pobelov, M. Mohos, K. Yoshida, V. Kolivoška, A. Avdic, A. Lugstein, E. Bertagnolli, K. Leonhardt, G. Denuault, B. Gollas and T. Wandlowski, *Nanotechnology* 2013, **24**, 115501.
- M. S. Hybertsen and L. Venkataraman, *Acc. Chem. Res.* 2016, **49**, 452.
- S. Aradhya and L. Venkataraman, *Nat. Nanotechnol.* 2013, **8**, 399.
- P. Chinwangso, A. C. Jamison and T. R. Lee, *Acc. Chem. Res.* 2011, **44**, 511.
- R. J. Davidson, D. C. Milan, O. A. Al-Owaedi, A. K. Ismael, R. J. Nichols, S. J. Higgins, C. J. Lambert, D. S. Yufit and A. Beeby, *RSC Adv.* 2018, **8**, 23585.
- M. Valášek, M. Lindner and M. Mayor, *Beilstein J. Nanotech.* 2016, **7**, 374.
- M. Valášek and M. Mayor, *Chem. Eur. J.* 2017, **23**, 13538.
- B. Singhana, S. Rittikulsittichai and T. R. Lee, *Langmuir* 2013, **29**, 561.
- B. Singhana, A. C. Jamison, J. Hoang and T. R. Lee, *Langmuir* 2013, **29**, 14108.
- T. Kitagawa, Y. Idomoto, H. Matsubara, D. Hobara, T. Kakiuchi, T. Okazaki and K. Komatsu, *J. Org. Chem.* 2006, **71**, 1362.
- T. Kitagawa, H. Matsubara, K. Komatsu, K. Hirai, T. Okazaki and T. Hase, *Langmuir* 2013, **29**, 4275.
- N. Hauptmann, L. Gross, K. Buchmann, K. Scheil, C. Schütt, F. L. Otte, R. Herges, C. Herrmann and R. Berndt, *New J. Phys.* 2015, **17**, 013012.
- Z. Wei, X. Wang, A. Borges, M. Santella, T. Li, J. K. Sørensen, M. Vanin, W. Hu, Y. Liu, J. Ulstrup, G. C. Solomon, Q. Chi, T. Bjørnholm, K. Nørgaard and B. W. Laursen, *Langmuir* 2014, **30**, 14868.
- S. Kuhn, U. Jung, S. Ulrich, R. Herges and O. Magnussen, *Chem. Commun.* 2011, **47**, 8880.
- K. Scheil, T. G. Gopakumar, J. Bahrenburg, F. Temps, R. J. Maurer, K. Reuter and R. Berndt, *J. Phys. Chem. Lett.* 2016, **7**, 2080.
- M. Valášek, K. Edelmann, L. Gerhard, O. Fuhr, M. Lukas and M. Mayor, *J. Org. Chem.* 2014, **79**, 7342.
- J. Šebera, V. Kolivoška, M. Valášek, J. Gasior, R. Sokolová, G. Mészáros, W. Hong, M. Mayor and M. Hromadová, *J. Phys. Chem. C* 2017, **121**, 12885.
- M. A. Karimi, S. G. Bahoosh, M. Valášek, M. Bürkle, M. Mayor, F. Pauly and E. Scheer, *Nanoscale* 2016, **8**, 10582.
- R. Sakamoto, Y. Ohirabaru, R. Matsuoka, H. Maeda, S. Katagiri and H. Nishihara, *Chem. Commun.* 2013, **49**, 7108.
- M. Lindner, M. Valášek, M. Mayor, T. Frauhammer, W. Wulfhekel and L. Gerhard, *Angew. Chem. Int. Ed.* 2017, **56**, 8290.
- M. Lindner, M. Valášek, L. Homberg, K. Edelmann, L. Gerhard, W. Wulfhekel, O. Fuhr, T. Wächter, M. Zharnikov, V. Kolivoška, L. Pospíšil, G. Mészáros, M. Hromadová and M. Mayor, *Chem. Eur. J.* 2016, **22**, 13218.
- Y. Ie, T. Hirose, H. Nakamura, M. Kiguchi, N. Takagi, M. Kawai and Y. Aso, *J. Am. Chem. Soc.* 2011, **133**, 3014.
- Y. Ie, K. Tanaka, A. Tashiro, S. K. Lee, H. R. Testai, R. Yamada, H. Tada and Y. Aso, *J. Phys. Chem. Lett.* 2015, **6**, 3754.
- T. Sebechlebská, J. Šebera, V. Kolivoška, M. Lindner, J. Gasior, G. Mészáros, M. Valášek, M. Mayor and M. Hromadová, *Electrochim. Acta* 2017, **258**, 1191.
- Š. Nováková Lachmanová, J. Šebera, V. Kolivoška, J. Gasior, G. Mészáros, G. Dupeyre, P. P. Lainé and M. Hromadová, *Electrochim. Acta* 2018, **264**, 301.
- G. Mészáros, Ch. Li, I. Pobelov and T. Wandlowski, *Nanotechnology* 2007, **18**, 424004.

Probabilistic Mapping of Asymmetric Molecular Junctions